R. & M. No. 3284

MINISTRY OF AVIATION

AERONAUTICAL RESEARCH COUNCIL
REPORTS AND MEMORANDA

Flutter of an All-Moving Tailplane

By

E. G. BROADBENT and MARGARET WILLIAMS

LONDON : HER MAJESTY'S STATIONERY OFFICE
1962
TEN SHILLINGS NET

Flutter of an All-Moving Tailplane

By

E. G. Broadbent and Margaret Williams

Communicated by the Director-General of Scientific Research (Air), Ministry of Supply

Reports and Memoranda No. 3284*

August, 1957

Summary.—Tailplane flutter is investigated theoretically for the following semi-rigid modes:

(i) tailplane bending, frequency ω_1

(ii) tailplane torsion, frequency ω_2

(iii) tailplane rotation, frequency ω_3

(iv) fuselage bending or torsion (according to symmetry), frequency ω_4.

The frequency ratios ω_2/ω_1 ; ω_3/ω_1 ; ω_4/ω_1, are varied and graphs of flutter speed against ω_3/ω_1 are given. The flutter speed drops sharply at low values of ω_3/ω_1 but it is probably the ratio ω_3/ω_4 that determines the position of the drop in flutter speed. Symmetric and antisymmetric results are included both for swept-back and unswept tailplanes. The effects of compressibility are excluded, apart from one isolated calculation, but this omission is not considered to have an important effect on the conclusions.

1. *Introduction.*—An important classical flutter problem on high-speed aircraft to-day is the flutter of all-moving surfaces, and in particular all-moving tailplanes. Current tendencies in design are for the longitudinal control to be effected by moving an all-moving tailplane, or possibly foreplane, without a separate elevator ; sometimes an elevator is retained for low-speed control but is locked at high speeds. It is this type of control (*i.e.*, without elevator) that is considered in the present paper, and the four degrees of freedom are bending and torsion of the tailplane, rotation of the tailplane, and either fuselage bending or fuselage torsion according to the type of symmetry represented.

One object of the work was to investigate any regions of dangerously low flutter speed that might occur locally, for example near to a frequency coincidence. The results show that such a region can exist, and suggest that the important frequency ratio is that between tailplane rotation and fuselage bending. As the calculations progressed it was desired to relate them, as closely as possible, to certain British prototype aircraft on which tailplane flutter was an important problem. This has led to the results covering a slightly less systematic range of parameters than might have been possible if the investigation had been one of pure research throughout, but the use of the Royal Aircraft Establishment Flutter Simulator has enabled a large number of results to be presented. The results are given roughly in the order in which they were obtained ; a swept tail was considered before an unswept tail because of the importance to a particular prototype.

Apart from one isolated calculation no allowance has been made for the effects of compressibility in this work. The reasons are, first, that the worst conditions may well be at high equivalent air speed and low altitude where the Mach number may not be very high, secondly

* Previously issued as R.A.E. Report No. Structures 226—A.R.C. 20,186.

the effect of compressibility at subsonic speeds is usually not important on this type of flutter (*see*, for example, the calculation reported in Section 5.3) and thirdly at supersonic speeds the aft shift in the aerodynamic centre is likely to be beneficial. At supersonic speeds in practice, however, the problem is likely to change completely with the possibility of negative aerodynamic damping that can lead to flutter which is not of the classical type.

2. *Symmetric Ternary Flutter.*—Tailplane flutter can be looked at in two ways ; either as binary flutter between a fuselage mode and tailplane rotation, and modified by the tailplane flexibilities, or as binary flexure-torsion flutter of the tailplane modified by fuselage bending and tailplane rotation. In the present paper the second outlook has been adopted, and since the tailplane rotational frequency has been chosen as the primary variable the first calculations carried out took account of the two tailplane flexibilities and of tailplane rotation in a set of ternary calculations. In practice the relative importance of the two principal binaries* will depend on the frequency ratios between the different degrees of freedom (as shown in Section 3.2), but the reason for regarding the flexure-torsion binary as the more important in the present investigation may briefly be given here.

The type of tail considered is an all-moving tailplane without elevator. In the past it has been more usual for an aircraft to be designed with an elevator as the primary longitudinal control, although tailplane rotation may be used for trimming purposes. In such a design the tailplane torsional stiffness is likely to be fixed by considerations of longitudinal control and stability, rather than flexure-torsion flutter of the tailplane, so that the critical speed for this type of flutter is likely to show a substantial margin over the design diving speed of the aircraft. When there is no elevator, however, twist of the tailplane is less important in longitudinal stability and control problems, so that the torsional stiffness may well be fixed by considerations of tailplane flutter. It follows that in these circumstances the margin of flexure-torsion flutter speed over design diving speed will be made as low as is consistent with safety in order to save weight. In general, therefore, a trimming tail, fitted with elevator, may be expected to have fuselage bending and tailplane rotation as its principal binary (or else be well removed from tailplane flutter altogether), whereas an all-moving tail without elevator may be expected to have a principal binary flutter consisting of tailplane bending and tailplane torsion.

2.1. *Assumptions.*—The geometry of the tailplane is shown in Fig. 1. The aspect ratio is higher than it would be in practice, but this fact should not alter any of the general conclusions. A high aspect ratio was chosen so that two-dimensional aerodynamic derivatives could be used without serious inconsistency, and in a research calculation it was thought better to use two-dimensional derivatives, rather than a rough three-dimensional approximation (more exact calculations would have taken too long) again for reasons of consistency. The aerodynamic assumptions, therefore, are that two-dimensional incompressible theory applies. The effect of Mach number on the flutter speeds is unlikely to be important, at any rate in subsonic flow, and it has not been generally investigated in the present work.

The tailplane is assumed to be pivoted about a swept-back axis along the quarter-chord, so that there is no aerodynamic stiffness to oppose the rotation of the tailplane. The three degrees of freedom are

(i) parabolic bending along the swept axis

$$z = c\eta^2 q_1$$

(ii) linear torsion about the flexural axis at the half-chord

$$\theta = \eta q_2$$

(iii) rigid rotation about the pivot axis at the quarter-chord

$$\theta = q_3$$

* The term principal binary is used to indicate the binary with the lowest associated flutter speed.

Here

z defines downward displacement

θ defines nose-up rotation of sections normal to the axis of sweepback

c is the chord

η is y/s

y is the distance of a section from the root, measured normal to the centreline

s is the distance from root to tip, measured normal to the centreline

q_1, q_2, q_3 are generalised co-ordinates, and the associated frequencies for pure structural deformation in each co-ordinate taken alone are denoted respectively by ω_1, ω_2 and ω_3.

The inertia axis is assumed to coincide with the flexural axis at the half-chord. The mass is given by

$$m/sc^2 = 1 \text{ lb/cu ft}$$

where m is the mass of the tailplane from root to tip, assumed to be uniformly distributed spanwise and with a chordwise radius of gyration of $\frac{1}{4}c$. The structural stiffnesses are varied. In addition to the basic calculations covered by these assumptions, two effects have been investigated. One of these is to change the pivot axis so as to place it normal to the aircraft centreline (shown as the alternative position in Fig. 1), the other is to move the inertia axis forward to 40 per cent of the chord, *i.e.*, to assume partial mass-balance.

2.2. *Results of the Calculations.*—The main variable in the calculation was the rotational frequency, ω_3, and the effect of changing ω_2 was also examined. The type of result obtained is shown in Fig. 2, where flutter speed is plotted against the frequency ratio ω_3/ω_1, where ω_1 is the tailplane bending frequency.* The flutter speed, v_c, is non-dimensional and has the form

$$v_c = Vc\sqrt{\frac{s\rho}{E_{11}}}$$

In Fig. 2 the ratio ω_2/ω_1 has the value 2, which is typical of full-scale experience. It can be seen that although the flutter speed drops a little with reducing ω_3 there is no sharp minimum in the curve and consequently no local region of particularly low flutter speed. The calculation was now repeated with the pivot axis changed so as to be normal to the aircraft centreline (*see* Fig. 1), but in this case the flutter speed scarcely changed at all with ω_3 ; the curve is shown on Fig. 2. A further attempt to find a region of low flutter speed was then made by repeating the calculation again with the inertia axis ahead of the flexural axis, *viz.*, at $0{\cdot}4c$ compared with $0{\cdot}5c$. In this case, also shown on Fig. 2, the binary flutter speed ($\omega_3 \rightarrow \infty$) is higher than before because of the mass-balancing effect but as ω_3 is reduced the flutter speed does pass through a minimum, which is lower than for the other curves, before rising again fairly steeply at still lower values of ω_3. The relatively high flutter speeds that were regularly obtained at very low values of ω_3 seemed unlikely to apply in practice, and it was decided to increase the scope of the calculations by introducing the fuselage degree of freedom.

3. *Symmetric Quaternary Flutter.*—3.1. *The Fuselage Freedom.*—Since this was a research investigation, the fuselage structure was not introduced directly into the calculation. It is assumed that the mode of fuselage bending is equivalent to rotation of the tailplane about a horizontal axis normal to the fuselage centreline and located two chord lengths ahead of the tailplane leading edge at the root (*see* Fig. 1). The structural stiffness of the mode is based on the natural frequency, ω_4, which is varied, so that the only effect of the fuselage structure is to

* In general ω_r is the natural frequency of mode r taken alone.

increase the direct inertia of mode 4, represented by the coefficient a_{44} ; this effect has been allowed for by doubling the contribution to $\hat{a}_{44}$ of the tailplane alone.* The four degrees of freedom allotted to the tailplane are now

(i) parabolic bending along the swept axis

$$z = c\eta^2 q_1$$

(ii) linear torsion about the flexural axis at the half-chord

$$\theta = \eta q_2$$

(iii) rigid rotation about the pivot axis at the quarter-chord

$$\theta = q_3$$

(iv) rigid rotation about an axis through the fuselage node normal to the centreline

$$\alpha = q_4, \text{ with } \hat{a}_{44} \text{ doubled.}$$

As there are now four degrees of freedom there are three significant frequency ratios, of which ω_3/ω_1 is varied from 0 to ∞ in all cases and the values of the other frequency ratios are shown in the table below.

$(\omega_2/\omega_1)^2$	2	4	4	4	8
$(\omega_4/\omega_1)^2$	$\frac{1}{2}$	$\frac{1}{2}$	1	2	2

The calculations described in this section and in all the later sections were performed on the R.A.E. Flutter Simulator.

3.2. *Results of the Calculation.*—A typical quaternary result is plotted in Fig. 3 and it can be seen that the flutter speed drops sharply at low values of ω_3. An explanation of the effect is provided by the other two curves shown on Fig. 3. On the one hand the ternary result (taken from Fig. 2) which is appropriate to a fuselage of infinite stiffness shows fair agreement with the flat part of the quaternary curve, and on the other hand the binary curve which is appropriate to a tailplane structure of infinite stiffness agrees well with the dip in the quaternary curve.

Fig. 4 shows the effect of varying the frequency ratios ω_2/ω_1 and ω_4/ω_1. As might be expected an increase in the tailplane torsional frequency is strongly beneficial except near the dip in the curves at low values of ω_3. Conversely variations in fuselage flexibility do not greatly influence the flutter speed except near the dip.

Some quaternary calculations were also carried out with the tailplane axis of rotation normal to the aircraft centreline as shown on Fig. 1. The results are shown in Fig. 5 where the principal effect of changing the axis can be seen to be the almost complete suppression of the dip in flutter speed. A probable reason for this is the very great increase in the tailplane moment of inertia about the pivot axis as indicated in the Appendix (Table A2). This has the effect that to achieve a given value of ω_3 the tailplane operating stiffness must be very much higher. The high aspect ratio of the tailplane is partly responsible for the large moment of inertia in this case and to that extent the calculation is unrepresentative of practice.

This is as far as the investigation was taken into symmetric flutter of a swept-back tailplane. It would seem that the sharpest minimum in flutter speed might be obtained by adding to the ternary with forward inertia axis (Fig. 3) a fuselage bending freedom such as resulted in the minima obtained in Fig. 5 ; it is, of course, possible that a different tailplane configuration would result in still lower minimum flutter speed.

4. *The Normal Mode Approach.*—If the routine procedure of a resonance test followed by flutter calculations is applied in the clearance of a new prototype with a flying tail, the modes obtained will not be those used in Sections 2 and 3, but will be resonance modes built up from

* The circumflex over a_{44} denotes the structural part of that coefficient (*see* List of Symbols).

combinations of those simple modes. In the absence of structural damping the resonance modes will be normal modes which can be readily calculated ; in practice small amounts of structural damping will not seriously affect the results. It was therefore decided to calculate the normal modes of the tailplane for a few particular values of the structural stiffnesses. For this purpose the deformability of the tailplane was assumed to be fully expressible in terms of the four semi-rigid modes used in the last section ; it follows that not more than four normal modes can be obtained and further that the flutter speed as calculated from all four normal modes should be identical with the corresponding flutter speed as calculated in the last section. The main purpose of this investigation, however, was to determine the effect of omitting one or more of the normal modes in the flutter calculations, as is discussed in Section 4.3 below.

4.1. *Calculation of the Normal Modes.*—The normal modes for the ternary (*i.e.*, fuselage rigid) were calculated by expanding the determinant and solving the characteristic equation for frequency. This was done for two values of the frequency ω_3, and the natural frequencies, Ω which were obtained are given in Table 1 below.

TABLE 1

Basic frequency ratios		Normal mode frequency ratios Ω/ω_1		
ω_2/ω_1	ω_3/ω_1	first (Ω_1/ω_1)	second	third
2	5	0·99	2·01	8·72
2	1	0·77	1·46	3·07

The modal shapes for these two sets of normal modes are given in Figs. 6 and 7, where the leading- and trailing-edge deflections are plotted in each case. The characteristic effect of sweepback is seen in Fig. 6a where the mode, which is primarily one of tailplane bending, shows considerably greater deflections of the trailing edge that the leading edge. In Fig. 7a (where ω_2/ω_1 is unity) this mode includes considerable tailplane rotation ; the coincident frequencies ($\omega_3 = \omega_1$) split into the pair of normal modes at frequency ratios of 0·77 and 1·46 with the familiar interchange of phase between the two.

The normal modes for the quaternaries (*i.e.*, including fuselage flexibility) were calculated from the ternary solutions using the escalator method in reverse[1]. The calculated frequencies for the cases considered are given in Table 2.

TABLE 2

Basic frequency ratios			Normal mode frequency ratios Ω/ω_1			
ω_2/ω_1	ω_3/ω_1	ω_4/ω_1	Ω_1/ω_1	Ω_2/ω_1	Ω_3/ω_1	Ω_4/ω_1
2	5	0·71	0·64	1·38	2·03	9·53
2	5	1·42	0·89	1·90	2·09	9·55
2	1	0·71	0·58	1·15	1·54	3·27
2	1	1·42	0·73	1·42	1·96	3·35

The modal shapes are plotted in Figs. 8, 9, 10, 11 and the phase changes of the component modes between one normal mode and the next can be clearly seen. In each case the normal mode of highest frequency is primarily a combination of tailplane torsion and tailplane rotation with the two constituents having opposite signs so that a torsional node occurs at about half span.

4.2. *Flutter Calculations using the Normal Modes.*—The next step was to carry out flutter calculations using the normal modes as generalised co-ordinates. Clearly the flutter speed obtained with all four normal modes should be identical with that obtained from the corresponding four assumed modes ; this comparison, together with flutter speeds obtained from smaller combinations of normal modes, is given in Tables 3, 4, 5 and 6 for the four cases of Table 2.

TABLE 3

Binaries			Ternaries			Quaternary		
D.O.F.	v	ω	D.O.F.	v	ω	v	ω	corresponds to row 1 of Table 2
1,2	>2·2		1,2,3	1·110	0·924	1·098	0·924	
1,3	1·302	0·698	1,2,4	>2·2				
1,4	>2·2		1,3,4	1·306	0·730			
2,3	1·176	0·870	2,3,4	1·170	0·850			
2,4	>2·2							
3,4	1·8	div*						
assumed mode calculation						1·142	0·90	

TABLE 4

Binaries			Ternaries			Quaternary		
D.O.F.	v	ω	D.O.F.	v	ω	v	ω	corresponds to row 2 of Table 2
1,2	1·384	0·860	1,2,3	1·140	0·785	1·134	0·805	
1,3	1·442	0·952	1,2,4	1·394	0·870			
1,4	>2·2		1,3,4	1·448	0·960			
2,3	1·75	div*	2,3,4	1·75	div			
2,4	>2·2							
3,4	>2·2							
assumed mode calculation						1·160	0·785	

TABLE 5

Binaries			Ternaries			Quaternary		
D.O.F.	v	ω	D.O.F.	v	ω	v	ω	corresponds to row 3 of Table 2
1,2	0·834	0·538	1,2,3	0·783	0·524	0·740	0·491	
1,3	1·368	0·698	1,2,4	0·796	0·512			
1,4	>2·2		1,3,4	1·396	0·705			
2,3	>2·2		2,3,4	1·2	div			
2,4	1·5	div*						
3,4	>2·2							
assumed mode calculation						0·760		

* Denotes steady divergence without oscillation

TABLE 6

Binaries			Ternaries			Quaternary		
D.O.F.	v	ω	D.O.F.	v	ω	v	ω	corresponds to row 4 of Table 2
1,2	0·846	0.648	1,2,3	0·834	0·64	0·803	0·64	
1,3	>2·2		1,2,4	0·806	0·67			
1,4	>2·2		1,3,4	>2·2				
2,3	1·3	div	2,3,4	1·3	div			
2,4	1·3	div						
3,4	>2·2							
assumed mode calculation						0·750		

As seen in the Tables 3, 4, 5 and 6 the flutter speeds obtained from all four normal modes are not identical with those obtained from the corresponding four assumed modes. The differences are attributed to the following factors :

(i) rounding-off errors in the simulator coefficients

(ii) random errors in the simulator solution

(iii) neglect of the structural cross dampings.

Item (iii) arises because the transformation to normal mode co-ordinates (*see* Appendix) strictly introduces cross dampings ; these were generally ignored, but in one case (that given in Table 4) the effect was investigated. The flutter speed for the assumed mode calculation was 2 per cent higher than that given by the normal mode calculation, but when appropriate cross dampings were included, the difference was decreased to $1\frac{1}{2}$ per cent.

4.3. *Application to Aircraft Clearance from Ground Resonance Tests.*—The purpose of this investigation was to see the effect on the flutter speed of omitting one or two normal modes. If two are omitted the flutter speed is increased considerably but when the fourth mode (*i.e.*, the mode of highest frequency) is omitted by itself the increase in flutter speed is small. This fact is of considerable importance in practice because the aircraft mode corresponding to the highest frequency normal modes of Tables 3 to 6 may be omitted. This can occur if the flutter calculations are based on measured resonance modes, in which case the highest frequency of the tests is limited by practical considerations. The difficulty is that the normal mode frequencies cover a much wider range than the arbitrary mode frequencies ; for example in Table 2, where the basic frequency ratios range from 1 to 2, the corresponding normal mode frequency ratios range from 0·73 to 3·35. This would mean that if the fundamental tailplane frequency of an aircraft were 20 c.p.s. (a typical value for a fighter) the frequency of mode 4 would be 92 c.p.s. and probably outside the test range. For a higher tailplane rotational stiffness (*see* Table 2) the frequency range is even greater. The actual errors in flutter speed (from Tables 3, 4, 5 and 6) caused by omitting the highest frequency modes are all less than 6 per cent.

In practice a ternary calculation may lead to greater errors than this because the degrees of freedom in reality are unrestricted, but it seems unlikely that modes outside the frequency range of ground resonance tests can have a major effect on the flutter speed.

5. *Results for an Unswept Tailplane.*—5.1. *Variation of Basic Frequency Ratios.*—The geometry of the unswept tailplane is shown in Fig. 12 ; the taper and aspect ratio, zero and 4 respectively, are the same as for the swept tailplane.

The assumed modes correspond with those for the swept tailplane, *viz.*,

(i) parabolic bending along the spanwise axis

$$z = c\eta^2 q_1$$

(ii) linear torsion about the flexural axis at the half-chord

$$\theta = \eta q_2 = \alpha$$

(iii) rigid rotation about the pivot axis at the quarter-chord

$$\theta = q_3 = \alpha$$

(iv) rigid rotation about the fuselage nodal point distant two chord lengths ahead of the tailplane leading edge

$$\alpha = q_4, \text{ with } \hat{a}_{44} \text{ doubled.}$$

It was soon apparent that the results were following the same trend as for the swept tailplane, so the opportunity was taken to cover more cases of frequency coincidence. Results are given for frequency ratios

$$\left.\begin{array}{ll} \omega_3/\omega_1 & \text{variable} \\ \omega_2/\omega_1 & 1{\cdot}0,\ \sqrt{2},\ 2{\cdot}0 \\ \omega_4/\omega_1 & 1/\sqrt{2} \qquad \sqrt{2} \end{array}\right\} \text{varied independently.}$$

The six graphs of v against ω_3/ω_1 for the six possible combinations of the frequency ratios ω_2/ω_1 and ω_4/ω_1 are given in Fig. 13. It can be seen that there are no very serious effects from frequency coincidences. In fact the greatest change in flutter speed along the curve occurs where the frequencies are most widely separated ; this result is expected in view of the change in form of the flutter between high and low values of ω_3/ω_1.

5.2. *Effect of Position of Fuselage Node.*—In the work discussed in all the earlier sections of this paper the fuselage node was assumed to be two chord lengths ahead of the tailplane leading edge. In the present section results are given for corresponding distances of one chord length and four chord lengths respectively. The results are given in Fig. 14 for two values of the frequency ratio ω_4/ω_1 in each case ; it can be seen that the position of the node has little effect on the shape of the curves (less than the change in frequency ratio ω_4/ω_1) but at high values of ω_3/ω_1 the more forward nodal point is favourable.

5.3. *A Result for High Mach Number.*—In one case the effect of using aerodynamic derivatives appropriate to a Mach number of 0·8 instead of zero was examined. The result is given in Fig. 15 ; the appropriate frequency ratios are

$$\omega_2/\omega_1 = 2{\cdot}0\ ; \qquad \omega_3/\omega_1 = 2{\cdot}0\ ;$$

and v_e is plotted against ω_4/ω_1. It can be seen that the flutter speed is only reduced by Mach number at low values of the fuselage frequency.

5.4. *The Effect of Structural Damping.*—In one case the possibility of raising the flutter speed by structural damping in mode 3 (tailplane rotation) was examined. For practical amounts of structural damping the gain in flutter speed is poor, as shown by the results given in Fig. 16. The frequency ratios are

$$\omega_2/\omega_1 = 2\ ; \qquad \omega_3/\omega_1 = 1{\cdot}0 \text{ and } \sqrt{2}\ ; \qquad \omega_4/\omega_1 = 1/\sqrt{2}$$

and flutter speed is plotted against structural damping expressed as a fraction of critical.

6. *Antisymmetric Flutter.*—In the antisymmetric calculations it is assumed that the first three arbitrary modes, represented by the co-ordinates q_1, q_2 and q_3 as given in Sections 2.1 and 5.1 are unchanged, and that only mode 4 is different. For mode 4 fuselage torsion is required instead of fuselage bending, and we assume the displacement in this mode to be given by

$$z = c\eta q_4 \; ; \qquad \alpha = 0.$$

The calculations have been carried out both for the swept and unswept tailplanes.

6.1. *Results for the Swept Tailplane.*—The flutter curves have the same general shape as for the symmetric calculations, and are given in Fig. 17. The dip in flutter speed at low values of ω_3/ω_1 is not quite so severe as in the symmetric case, and is greatest when the fuselage torsional frequency coincides with the tailplane bending frequency ($\omega_4/\omega_1 = 1{\cdot}0$) which differs from the symmetric result. Rather higher values of the fuselage torsional frequency were chosen than of the fuselage bending frequency, because this is generally (although not always) in accordance with practice. The values chosen are

$$\omega_4/\omega_1 = 1{\cdot}0,\ 2{\cdot}0 \text{ and } 4{\cdot}0 \; ; \qquad \omega_2/\omega_1 = 2{\cdot}0 \text{ throughout.}$$

6.2. *Results for the Unswept Tailplane.*—Again the curves follow the same pattern. The results are given in Fig. 18 for frequency ratios :

$$\omega_4/\omega_1 = 1{\cdot}18,\ 1{\cdot}65,\ 2{\cdot}36,\ 3{\cdot}33 \; ; \qquad \omega_2/\omega_1 = 2 \text{ throughout.}$$

The dip at low values of ω_3/ω_1 is in this case rather more severe than the symmetric and is greatest at high values of the fuselage torsional frequency.

7. *Remarks on the Flutter of Foreplanes.*—It will be apparent that many of the results obtained for flutter of tailplanes will apply qualitatively to foreplanes also. Ternary results (fuselage rigid) and antisymmetric results will be unchanged as all the arbitrary modes are identical in these calculations. The symmetric calculation with flexible fuselage will differ on account of the reversal in sign of the incidence in the fuselage bending mode. One effect of this is to change the direct aerodynamic stiffness c_{44} from positive to negative and thus to introduce the possibility of divergence. Apart from this the results for flutter will be modified slightly but in view of the unchanged antisymmetric picture there is unlikely to be much improvement. Body freedom flutter of the canard layout is a serious possibility, but in this type of flutter flexibility of the foreplane plays only a minor role, so that the subject is outside the scope of the present paper.

8. *Conclusions.*—The problem of tailplane flutter has been investigated on the basis of varying appropriate frequency ratios. It is considered that the use of four arbitrary modes, *viz.*,

(i) tailplane bending

(ii) tailplane torsion

(iii) tailplane rotation

(iv) fuselage bending or torsion according to symmetry

are sufficient to embrace any likely form of flutter. An important conclusion is that the *three* normal modes of lowest frequency are sufficient to give a reliable flutter speed.

The flutter curves are all of the same general shape, whether for symmetric or antisymmetric, swept or unswept cases, although a change in the pivot axis for a swept tail can lead to appreciable modification of the results. At low values of the tailplane rotational frequency the flutter speed drops sharply as flexure torsion flutter is overridden by (fuselage-bending)-(tailplane-rotation) flutter. Clearly, this region should be avoided in practice by the use of high operating stiffness of the tailplane. One cannot generalise as to whether symmetric or antisymmetric flutter is the worse, and each must be examined in specific cases with the relative frequency ratios probably being the deciding feature.

LIST OF SYMBOLS

a_{rs}	=	$\hat{a}_{rs} + \bar{a}_{rs}$
$\hat{a}_{rs}$		A typical structural inertia coefficient
$\bar{a}_{rs}$		A typical aerodynamic inertia coefficient
b_{rs}		A typical aerodynamic damping coefficient
c_{rs}		A typical aerodynamic stiffness coefficient
d_{rs}		A typical structural damping coefficient
e_{rs}		A typical structural stiffness coefficient
ω_r		Frequency of mode r
V		Flutter speed
v_c		Non-dimensional flutter speed
ρ		Air density
hc		Distance of flexural axis ahead of leading edge
c		Tailplane chord
s		Tailplane semi-span
z		Defines downward displacement
α		Defines nose-up rotation of sections parallel to the line of flight
θ		Defines nose-up rotation of sections normal to the axis of sweepback
η	=	y/s
y		Distance of a section from the root, measured normal to the centreline
q_1, q_2, q_3, q_4		Generalised co-ordinates
m		Mass of the tailplane from root to tip

REFERENCE

No.	*Author*	*Title, etc.*
1	Joseph Morris . .	*The Escalator method in engineering vibration problems.* Published by: Chapman and Hall, Ltd. 1947.

APPENDIX

Tables of Flutter Coefficients

TABLE A1

Scaled Coefficients for Swept Tailplane with the Original Four Degrees of Freedom

Degrees of freedom :

(1) Parabolic bending along the swept axis

(2) Linear torsion about the flexural axis at the half-chord

(3) Rigid rotation about the pivot axis at the quarter-chord

(4) Rigid rotation about the fuselage node (axis normal to centreline).

Time constant	1	1	4	$\frac{1}{2}$
a	1110	387	769	272
b	121	387	41	50
c	80	849	15	42
e	397			
a	27	380	117	3
b	−11	76	3	−8
c	−15	−166	−3	−9
e		$555R$		
a	230	500	415	81
b	12	166	17	4
c	0	0	0	0
e			$30 \cdot 8r$	
a	1110	177	1110	759
b	133	396	62	81
c	101	1110	27	74
e				$1110t$

Structural dampings were included in the leading diagonal terms of this table (and all subsequent tables), as $\frac{1}{2}$ per cent of critical damping.

$$e.g.,\ d_{11} = 0 \cdot 01 \sqrt{(1110 \times 397)} = 7, \text{ and similarly for } d_{22},\ d_{33} \text{ and } d_{44}$$

The variations of the stiffnesses in modes 2, 3, and 4 and their effect on the flutter speed are shown in Figs. 4a, b and c.

TABLE A2

Scaled Coefficients for Swept Tailplane with the Pitching Axis Normal to the Aircraft Centreline

(as shown in Fig. 1)

Modes 1, 2 and 4 as in Table A1.

Time constant	1	1	4	$\frac{1}{2}$
a			1110	
b			32	
c			6	
e				
a			39	
b			−2	
c			−1	
e				
a	471	234	499	123
b	50	182	14	20
c	32	342	2	16
e			$2 \cdot 4r$	
a			1180	
b			40	
c			10	
e				

The moment of inertia of the tailplane about its hinge-line a_{33}, is increased in the ratio 15·594:1. This is not immediately obvious from Tables A1 and A2 as the scaling factors on the third row and column in each case are different. The variations of the stiffnesses in modes 2, 3 and 4 and their effect on the flutter speed are shown in Fig. 5.

TABLE A3

Scaled Coefficients for Swept Tailplane with Calculated Four Normal Modes for Particular Values of the Structural Stiffnesses

The values of the structural stiffnesses correspond in this case to the following frequency ratios :

$$\frac{\omega_2}{\omega_1} = 2, \qquad \frac{\omega_3}{\omega_1} = 5, \qquad \frac{\omega_4}{\omega_1} = 1{\cdot}43$$

Time constant	$\frac{1}{2}$	1	1	4
a	976			
b	206	−148	135	5
c	298	−299	334	7
e	1110			
a		856		
b	56	92	−93	−36
c	191	−184	221	−11
e		1110		
a			709	
b	−67	−41	81	−17
c	−168	172	−186	−11
e			1110	
a				543
b	− 7	1	− 3	19
c	−12	12	−14	0
e				1110

The results are given in Table 4 of the main text which shows that the flutter speed gives good agreement with that obtained from the assumed mode calculation.

The normal modes for the ternary were calculated by expanding the determinant and solving the characteristic equation for frequency. The normal modes of the quaternary were then calculated from these using the escalator method in reverse in terms of variable frequency ratio. The matrix transformation $[q]\ [U]\ [q']$ was then carried out to obtain the new coefficients, where $[U]$ is the matrix of coefficients given in Table A1 for the corresponding values of the stiffnesses, *viz.*, in this case

$$\left.\begin{aligned} e_{22} &= 555 \\ e_{33} &= 232 \\ e_{44} &= 2220 \end{aligned}\right\}$$

$[q']$ is the square matrix of the four modal columns obtained from the four values of the frequency and $[q]$ its transpose. The modal shapes are plotted in Fig. 9.

The effect of the transformation on the structural dampings would be to introduce cross dampings, but as these were very small they were ignored. In fact for the case given in Table A3 they were later included in order to see what effect they would have on the flutter speed and the effect was an increase of less than 1 per cent.

TABLE A4

Scaled Coefficients for Swept Tailplane with Fuselage Torsion as the Fourth Degree of Freedom

Modes 1, 2 and 3 as in Table A1.

Time constant	1	1	4	1
a				1292
b				109
c				23
a				0
b				−22
c				− 5
a				278
b				0
c				0
a	412	0	296	775
b	51	126	17	53
c	38	413	8	11
e				$277 \cdot 5t$

The results of varying the stiffness in mode 4 for $\omega_2/\omega_1 = 2 \cdot 0$ are shown in Fig. 15, where v is plotted against ω_3/ω_1.

TABLE A5

Scaled Coefficients for Unswept Tailplane with the Original Four Degrees of Freedom

Degrees of freedom as for swept tailplane (*see* Table A1).

Time constant	1	1	2	$\frac{1}{2}$
a	1108	0	523	577
b	157	126	85	184
c	33	413	82	208
e	400			
a	0	594	505	56
b	−98	126	26	−100
c	−21	−276	−62	−156
e		857		
a	392	378	762	415
b	0	134	76	34
c	0	0	0	0
e			1101	
a	577	56	553	1065
b	74	90	83	160
c	16	233	69	176
e				754

The variations of the stiffnesses in modes 2, 3 and 4 and their effect on the flutter speed are shown in Fig. 13. The values of the structural stiffnesses given in the above table correspond to the following frequency ratios :

$$\omega_2/\omega_1 = 2{\cdot}0 \qquad \omega_3/\omega_1 = 4{\cdot}0 \qquad \omega_4/\omega_1 = 1/\sqrt{2}$$

TABLE A6

Scaled Coefficients for Unswept Tailplane with Fuselage Torsion as the Fourth Degree of Freedom

Modes 1, 2 and 3 as in Table A5.

Time constant	1	1	2	$\frac{1}{4}$
a				623
b				352
c				304
e				
a				0
b				−236
c				−192
e				
a				265
b				0
c				0
e				
a	623	0	1059	550
b	88	75	171	212
c	19	248	166	176
e				794

The results of varying the stiffness in mode 4 for $\omega_2/\omega_1 = 2{\cdot}0$ are shown in Fig. 16, where v_c is plotted against ω_3/ω_1. The value of e_{44} given in the table corresponds to a frequency ratio $\omega_4/\omega_1 = 0{\cdot}5$.

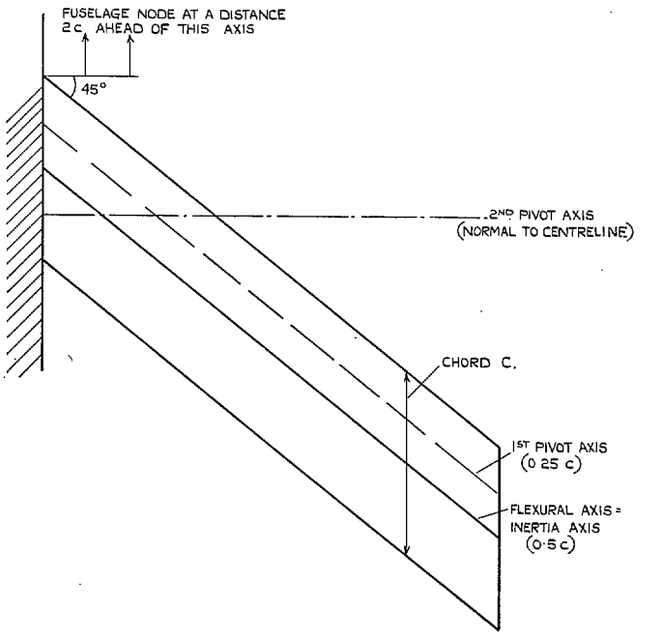

FIG. 1. General arrangement of swept-back tailplane.

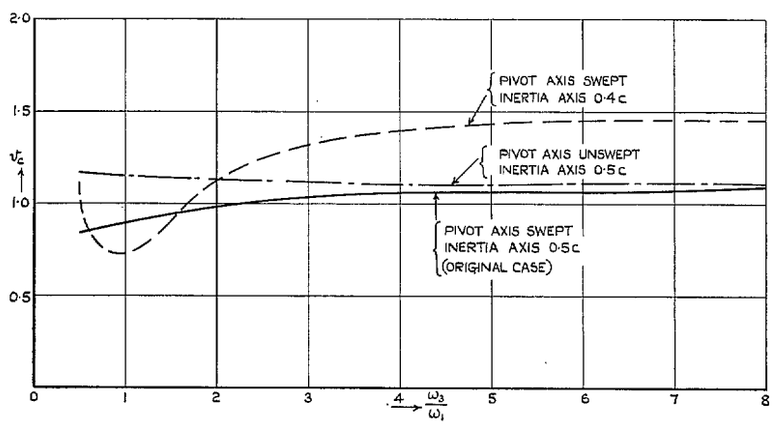

FIG. 2. v_e against ω_3/ω_1 : fuselage rigid : swept tailplane.

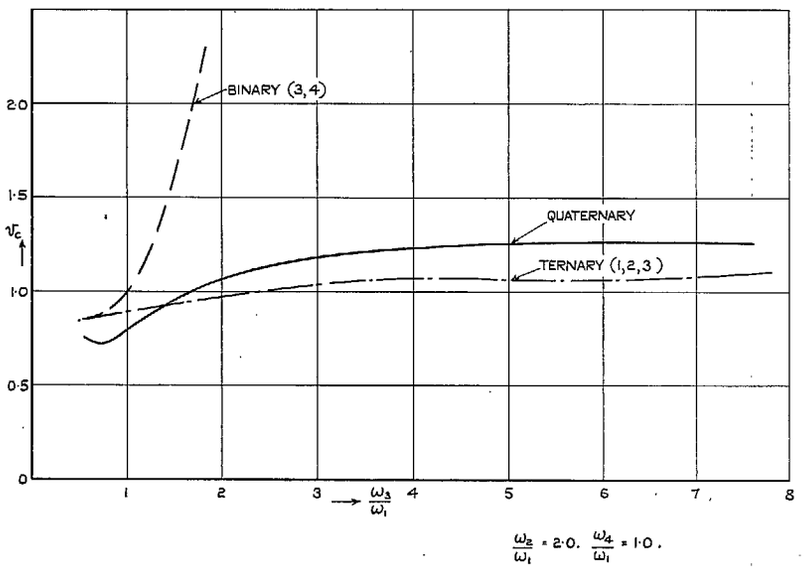

FIG. 3. v_c against ω_3/ω_1 : fuselage flexible : comparison with binary and ternary : swept tailplane.

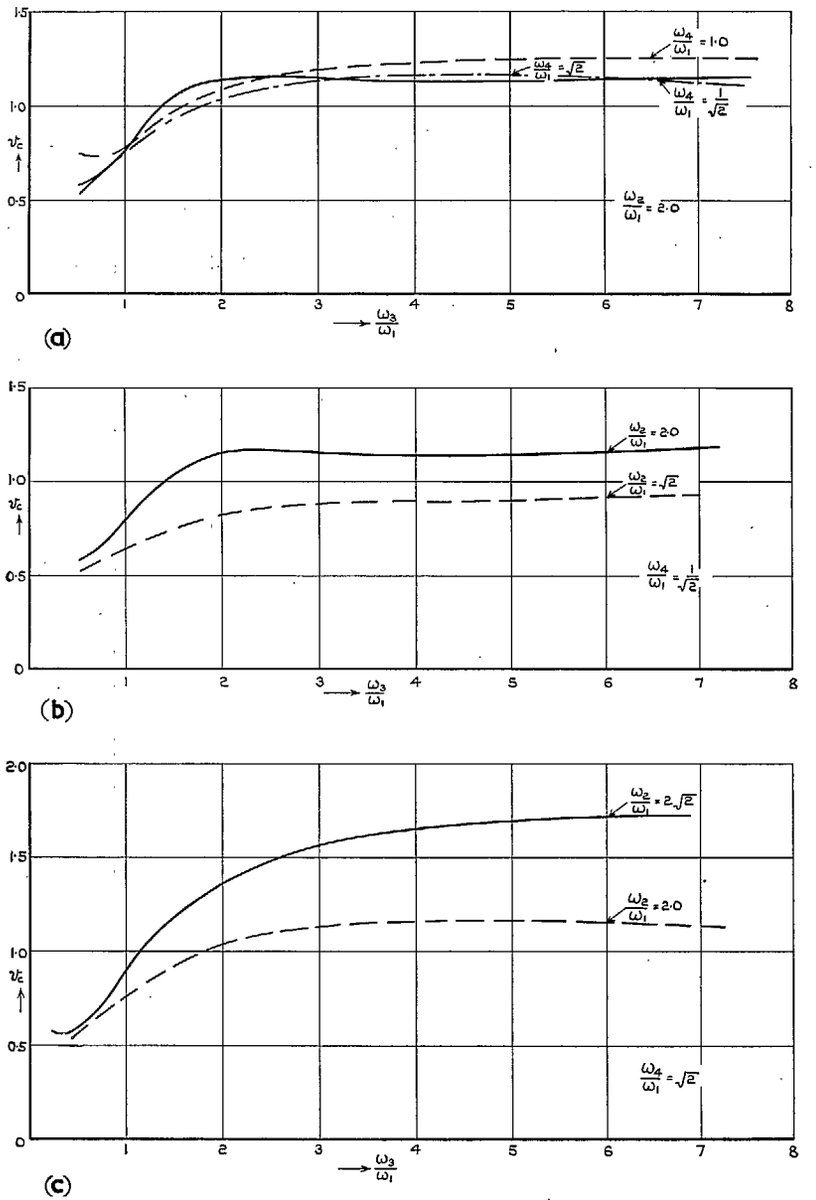

FIGS. 4a to c. v against ω_3/ω_1 for different values of ω_2/ω_1 and ω_4/ω_1 : swept tailplane.

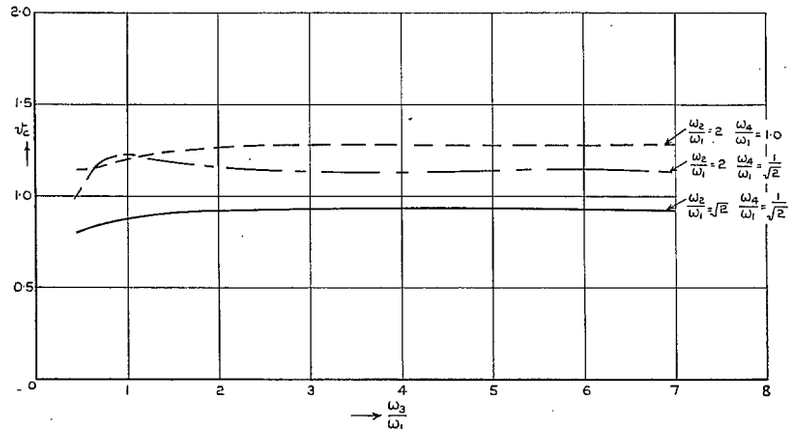

FIG. 5. v_e against ω_3/ω_1 : swept tailplane : pivot axis normal to centreline.

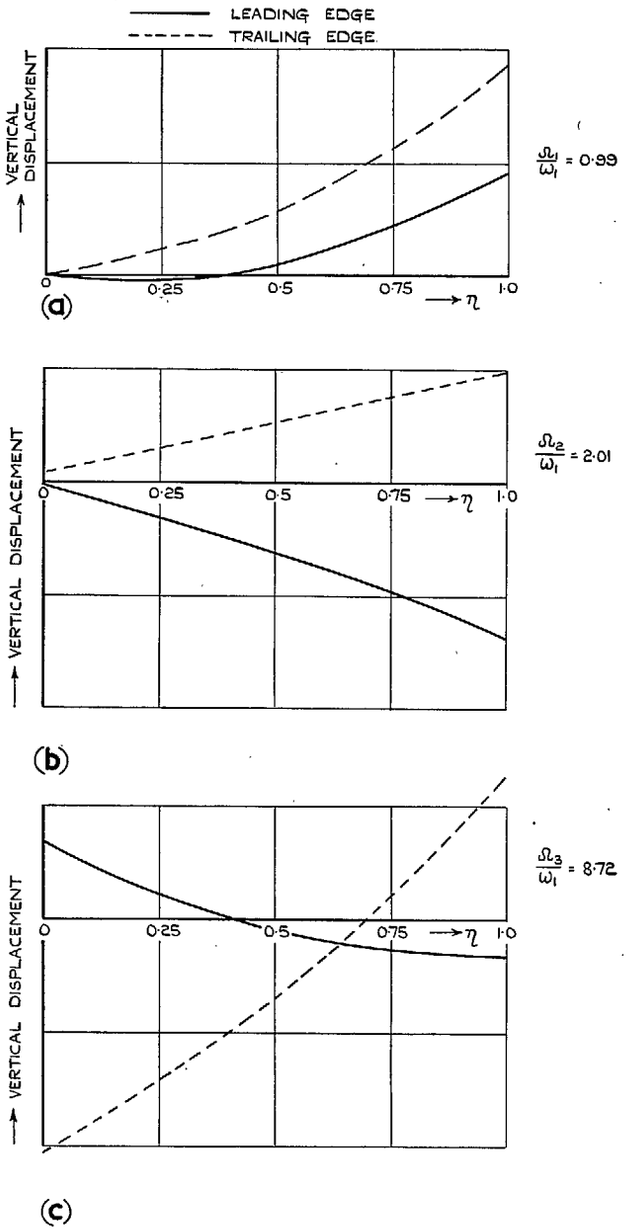

FIGS. 6a to c. Normal modes : $\omega_2/\omega_1 = 2{\cdot}0$; $\omega_3/\omega_1 = 5{\cdot}0$; fuselage rigid.

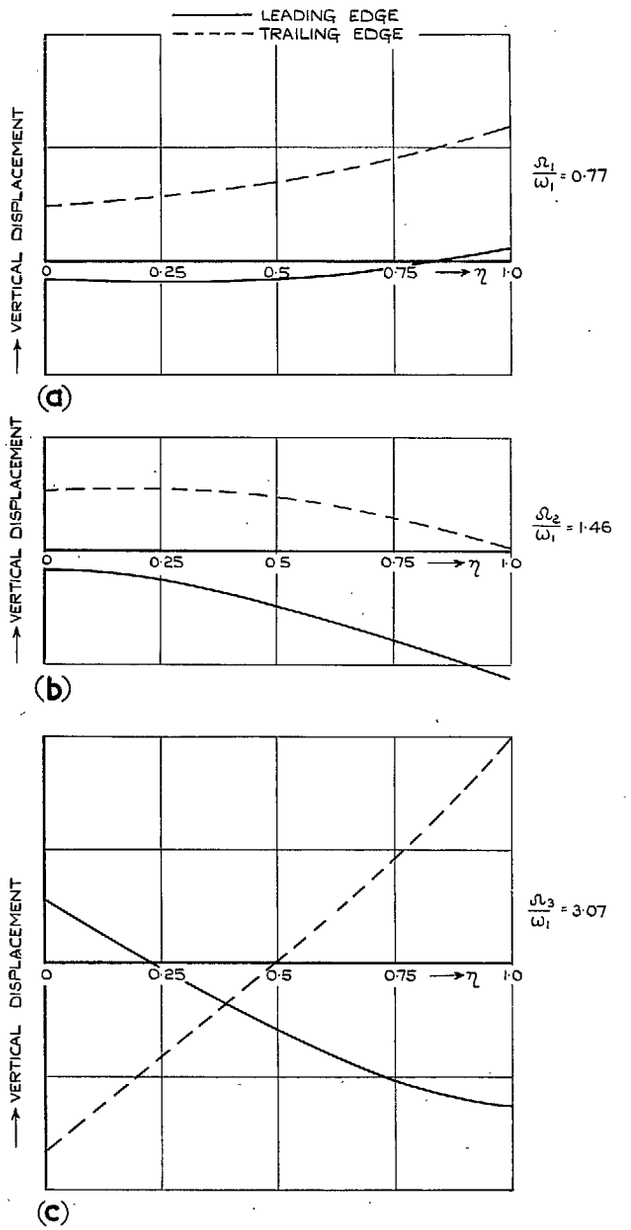

FIGS. 7a to c. Normal modes : $\omega_2/\omega_1 = 2{\cdot}0$; $\omega_3/\omega_1 = 1{\cdot}0$; fuselage rigid.

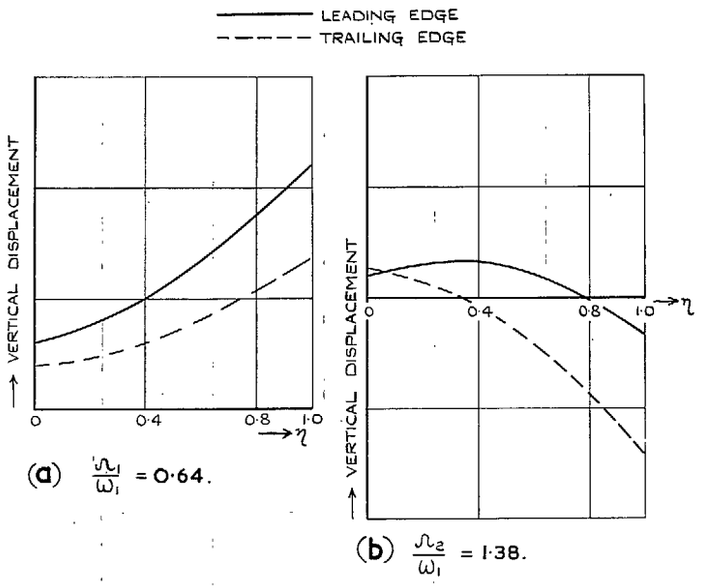

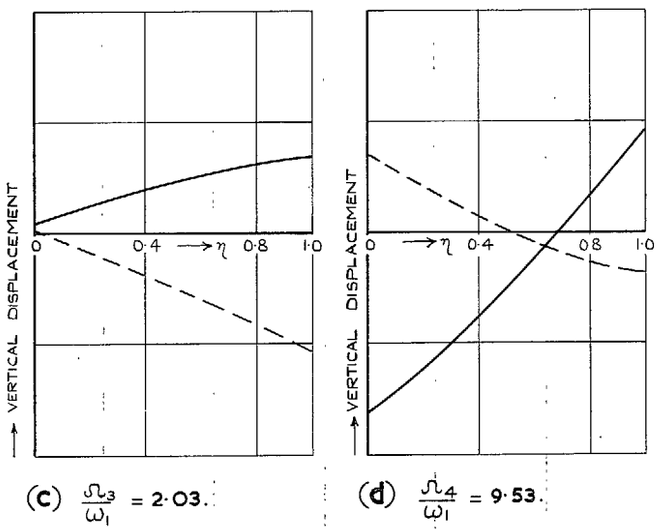

FIGS. 8a to d. Normal modes : $\omega_2/\omega_1 = 2{\cdot}0$; $\omega_3/\omega_1 = 5{\cdot}0$; $\omega_4/\omega_1 = 1/\sqrt{2}$.

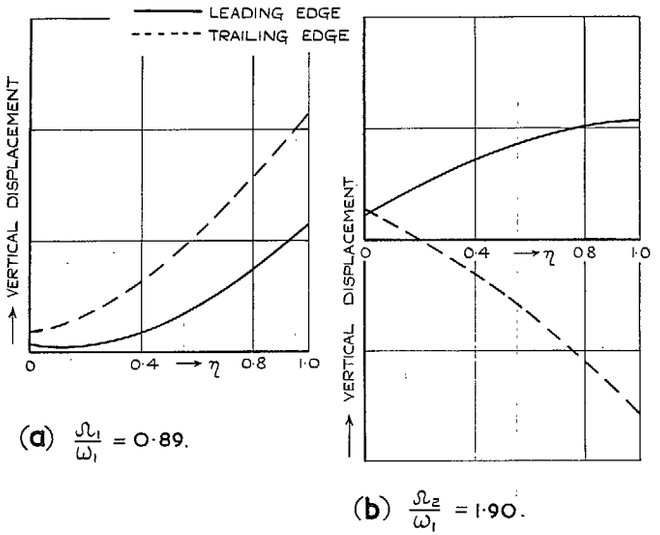

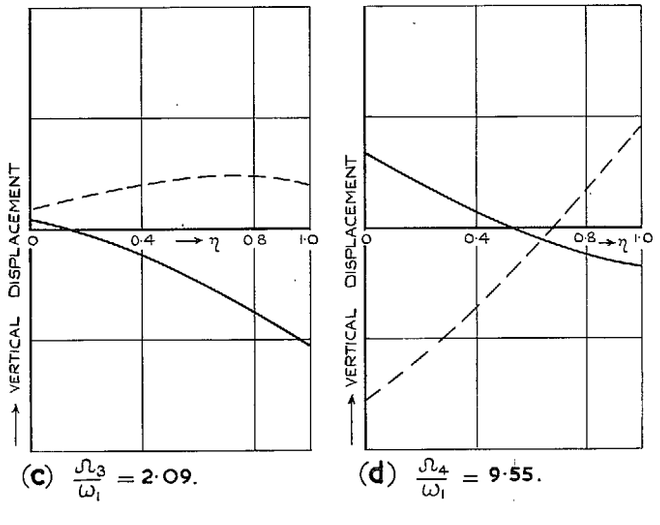

FIGS. 9a to d. Normal modes : $\omega_2/\omega_1 = 2{\cdot}0$; $\omega_3/\omega_1 = 5{\cdot}0$; $\omega_4/\omega_1 = \sqrt{2}$.

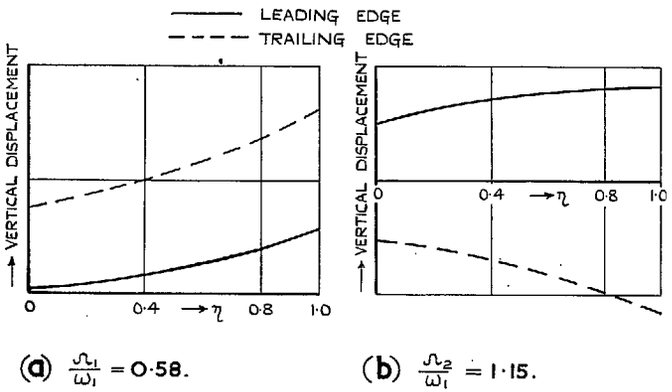

(a) $\frac{\Omega_1}{\omega_1} = 0{\cdot}58$. (b) $\frac{\Omega_2}{\omega_1} = 1{\cdot}15$.

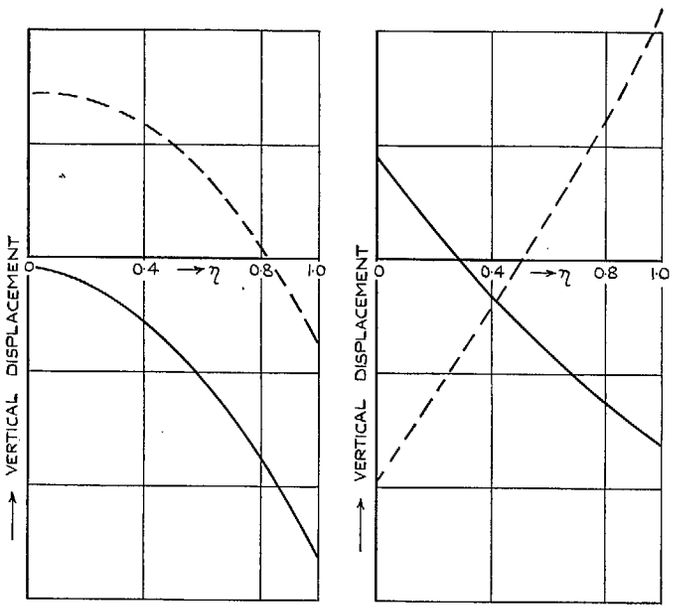

(c) $\frac{\Omega_3}{\omega_1} = 1{\cdot}54$. (d) $\frac{\Omega_4}{\omega_1} = 3{\cdot}27$.

FIGS. 10a to d. Normal modes : $\omega_2/\omega_1 = 2{\cdot}0$; $\omega_3/\omega_1 = 1{\cdot}0$; $\omega_4/\omega_1 = 1/\sqrt{2}$.

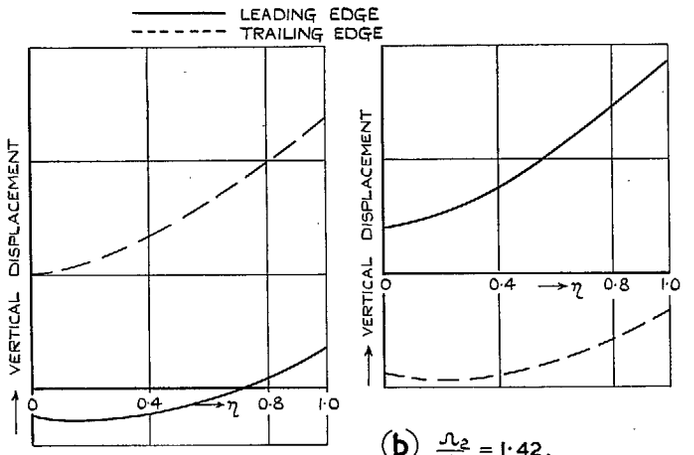

(a) $\frac{\Omega_1}{\omega_1} = 0{\cdot}73$. (b) $\frac{\Omega_2}{\omega_1} = 1{\cdot}42$.

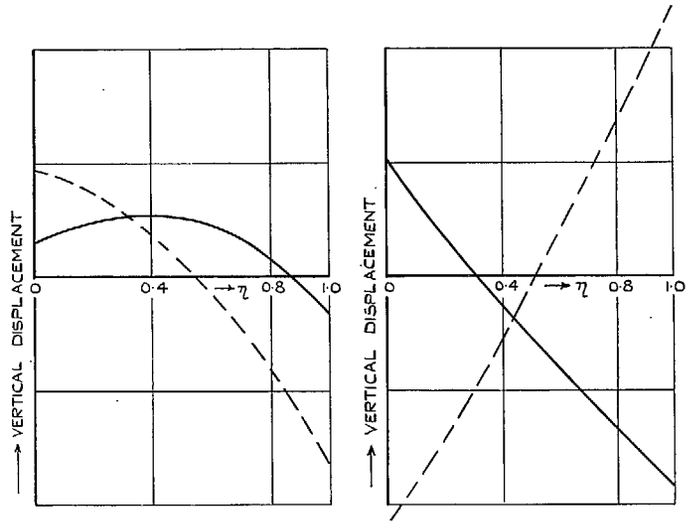

(c) $\frac{\Omega_3}{\omega_1} = 1{\cdot}96$. (d) $\frac{\Omega_4}{\omega_1} = 3{\cdot}35$.

FIGS. 11a to d. Normal modes : $\omega_2/\omega_1 = 2{\cdot}0$; $\omega_3/\omega_1 = 1{\cdot}0$; $\omega_4/\omega_1 = \sqrt{2}$.

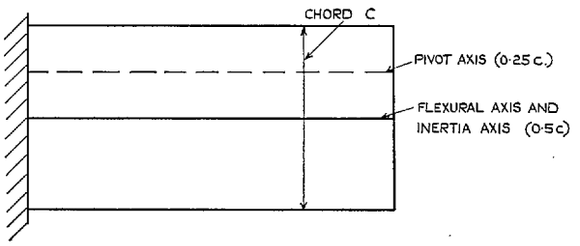

FIG. 12. General arrangement of unswept tailplane.

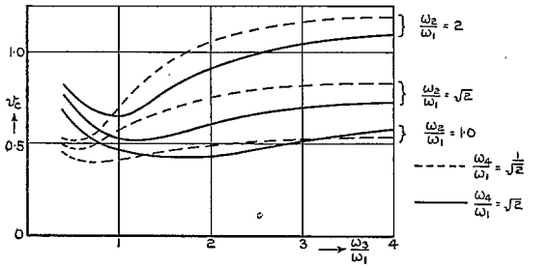

FIG. 13. v_c against ω_3/ω_1; ω_2/ω_1 and ω_4/ω_1 varied: unswept tailplane.

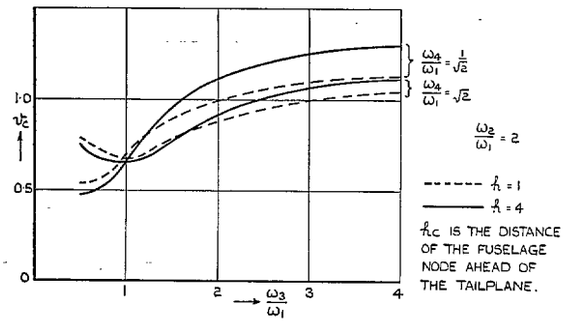

FIG. 14. v_c against ω_3/ω_1: fuselage node varied: unswept tailplane.

(85154) Wt. 62/1876 K.5 8/62 Hw.

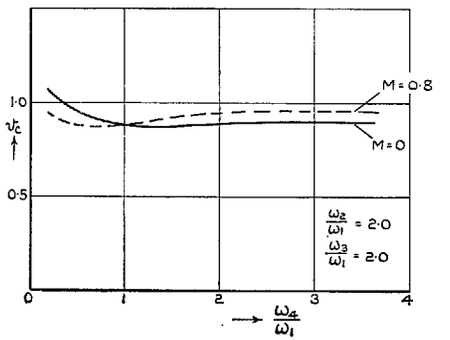

FIG. 15. v_c against ω_4/ω_1 : comparison between $M = 0$ and $M = 0{\cdot}8$.

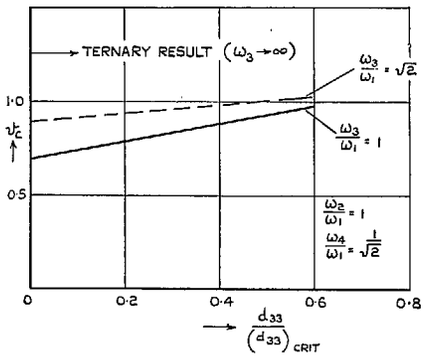

FIG. 16. v_c against structural damping in the tailplane rotational mode.

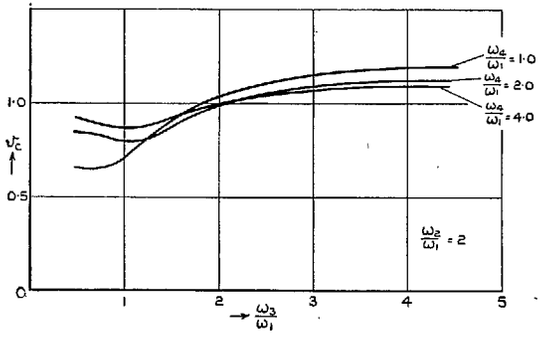

FIG. 17. v_c against ω_3/ω_1 : antisymmetric fuselage mode : swept tailplane.

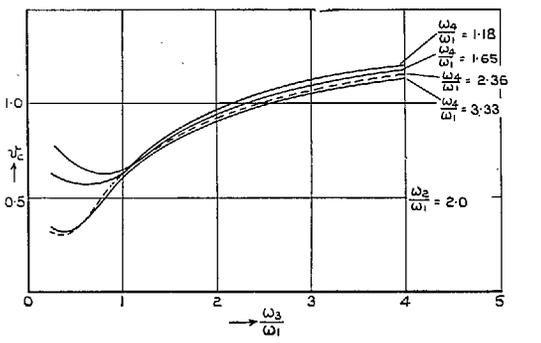

FIG. 18. v_c against ω_3/ω_1 : antisymmetric fuselage mode : unswept tailplane.

Publications of the Aeronautical Research Council

ANNUAL TECHNICAL REPORTS OF THE AERONAUTICAL RESEARCH COUNCIL (BOUND VOLUMES)

1942 Vol. I. Aero and Hydrodynamics, Aerofoils, Airscrews, Engines. 75*s.* (post 2*s.* 9*d.*)
Vol. II. Noise, Parachutes, Stability and Control, Structures, Vibration, Wind Tunnels. 47*s.* 6*d.* (post 2*s.* 3*d.*)

1943 Vol. I. Aerodynamics, Aerofoils, Airscrews. 80*s.* (post 2*s.* 6*d.*)
Vol. II. Engines, Flutter, Materials, Parachutes, Performance, Stability and Control, Structures. 90*s.* (post 2*s.* 9*d.*)

1944 Vol. I. Aero and Hydrodynamics, Aerofoils, Aircraft, Airscrews, Controls. 84*s.* (post 3*s.*)
Vol. II. Flutter and Vibration, Materials, Miscellaneous, Navigation, Parachutes, Performance, Plates and Panels, Stability, Structures, Test Equipment, Wind Tunnels. 84*s.* (post 3*s.*)

1945 Vol. I. Aero and Hydrodynamics, Aerofoils. 130*s.* (post 3*s.* 6*d.*)
Vol. II. Aircraft, Airscrews, Controls. 130*s.* (post 3*s.* 6*d.*)
Vol. III. Flutter and Vibration, Instruments, Miscellaneous, Parachutes, Plates and Panels, Propulsion. 130*s.* (post 3*s.* 3*d.*)
Vol. IV. Stability, Structures, Wind Tunnels, Wind Tunnel Technique. 130*s.* (post 3*s.* 3*d.*)

1946 Vol. I. Accidents, Aerodynamics, Aerofoils and Hydrofoils. 168*s.* (post 3*s.* 9*d.*)
Vol. II. Airscrews, Cabin Cooling, Chemical Hazards, Controls, Flames, Flutter, Helicopters, Instruments and Instrumentation, Interference, Jets, Miscellaneous, Parachutes. 168*s.* (post 3*s.* 3*d.*)
Vol. III. Performance, Propulsion, Seaplanes, Stability, Structures, Wind Tunnels. 168*s.* (post 3*s.* 6*d.*)

1947 Vol. I. Aerodynamics, Aerofoils, Aircraft. 168*s.* (post 3*s.* 9*d.*)
Vol. II. Airscrews and Rotors, Controls, Flutter, Materials, Miscellaneous, Parachutes, Propulsion, Seaplanes, Stability, Structures, Take-off and Landing. 168*s.* (post 3*s.* 9*d.*)

1948 Vol. I. Aerodynamics, Aerofoils, Aircraft, Airscrews, Controls, Flutter and Vibration, Helicopters, Instruments, Propulsion, Seaplane, Stability, Structures, Wind Tunnels. 130*s.* (post 3*s.* 3*d.*)
Vol. II. Aerodynamics, Aerofoils, Aircraft, Airscrews, Controls, Flutter and Vibration, Helicopters, Instruments, Propulsion, Seaplane, Stability, Structures, Wind Tunnels. 110*s.* (post 3*s.* 3*d.*)

Annual Reports of the Aeronautical Research Council—
1939–48 3*s.* (post 6*d.*) 1949–54 5*s.* (post 5*d.*)

Index to all Reports and Memoranda published in the Annual Technical Reports, and separately—
April, 1950 – – – – R. & M. 2600 (out of print)

Published Reports and Memoranda of the Aeronautical Research Council—

Between Nos. 2351–2449	R. & M. No. 2450 2*s.* (post 3*d.*)
Between Nos. 2451–2549	R. & M. No. 2550 2*s.* 6*d.* (post 3*d.*)
Between Nos. 2551–2649	R. & M. No. 2650 2*s.* 6*d.* (post 3*d.*)
Between Nos. 2651–2749	R. & M. No. 2750 2*s.* 6*d.* (post 3*d.*)
Between Nos. 2751–2849	R. & M. No. 2850 2*s.* 6*d.* (post 3*d.*)
Between Nos. 2851–2949	R. & M. No. 2950 3*s.* (post 3*d.*)
Between Nos. 2951–3049	R. & M. No. 3050 3*s.* 6*d.* (post 3*d.*)
Between Nos. 3051–3149	R. & M. No. 3150 3*s.* 6*d.* (post 3*d.*)

HER MAJESTY'S STATIONERY OFFICE

York House, Kingsway, London W.C.2; 423 Oxford Street, London W.1; 13a Castle Street, Edinburgh 2; 39 King Street, Manchester 2; 35 Smallbrook, Ringway, Birmingham 5; 109 St. Mary Street, Cardiff; 50 Fairfax Street, Bristol 1; 80 Chichester Street, Belfast 1, *or through any bookseller.*

S.O. Code No. 23-3284